



ISSN 0022-4804

Volume 140

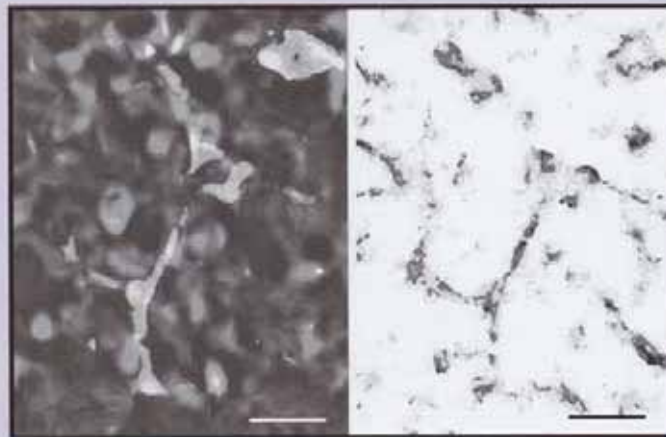
Number 2

June 15, 2007

JSR

Journal of
Surgical Research

**Presented at 2nd
Annual Academic
Surgical Congress,
Phoenix, Arizona
February 6–9, 2007**



Official Publication of the
Association for Academic Surgery

Full-Text and Submit Manuscripts:
www.JournalofSurgicalResearch.com

Dual-Color Imaging of Angiogenesis and Its Inhibition in Bone and Soft Tissue Sarcoma

Katsuhiro Hayashi, M.D.,*†‡ Kensuke Yamauchi, M.D.,‡ Norio Yamamoto, M.D.,‡ Hiroyuki Tsuchiya, M.D.,‡ Katsuro Tomita, M.D.,‡ Yasuyuki Amoh, M.D.,† Robert M. Hoffman, Ph.D.,*† and Michael Bouvet, M.D.*¹

*Department of Surgery, University of California San Diego, San Diego, California; †AntiCancer, Inc., San Diego, California; ‡Department of Orthopedic Surgery, School of Medicine, Kanazawa University, Kanazawa, Japan

Submitted for publication August 20, 2006

Background. Angiogenesis is a critical step in tumor growth, progression, and metastasis. Soft tissue and bone sarcoma are resistant to most therapeutic approaches. Angiogenesis of these tumors may be an effective target. We hypothesized that we could inhibit tumor growth by targeting angiogenesis in a mouse model of sarcoma. We demonstrate in this report, using powerful color-coded fluorescent imageable tumor-host models, the onset of angiogenesis of these sarcomas and its inhibition.

Materials and methods. Transgenic mice were used as the host in which green fluorescent protein (GFP) is driven by a regulatory element of the stem cell marker nestin (ND-GFP). Nascent blood vessels express ND-GFP in this model. We visualized, by dual-color fluorescence imaging, angiogenesis of sarcoma formed by the HT-1080 human fibrosarcoma cell line expressing red fluorescent protein (RFP) in the ND-GFP mice. Tumor cells were injected into either the muscle or the bone.

Results. Nestin was highly expressed in proliferating endothelial cells and nascent blood vessels in the growing tumors, including the surrounding tissues. Immunohistochemical staining showed that CD31 colocalized in ND-GFP-expressing nascent blood vessels. The density of nascent blood vessels in the tumor was readily quantitated. The mice were given daily i.p. injections of 5 mg/kg of doxorubicin after implantation of tumor cells. Doxorubicin significantly decreased the mean nascent blood vessel density in the tumors as well as decreased tumor volume.

Conclusion. The dual-color model of the ND-GFP nude mouse and RFP sarcoma cells is useful for the

visualization and quantitation of bone and soft tissue tumor angiogenesis and evaluation of angiogenic inhibitors for such tumors. These data suggest targeting angiogenesis of sarcomas as a promising clinical approach. © 2007 Elsevier Inc. All rights reserved.

Key Words: GFP; RFP; nestin; nascent blood vessels; HT1080; doxorubicin.

INTRODUCTION

We report here a new imageable model of angiogenesis of bone and soft tissue tumor sarcoma, tumor types that are highly aggressive and resistant to most current treatment modalities. A further understanding of angiogenesis of this tumor type should provide potential targets for novel and effective therapy.

Angiogenesis is a critical step in tumor growth, progression, and metastasis and, therefore, is a target in worldwide drug discovery programs. The discovery and evaluation of antiangiogenic substances have previously relied on *in vivo* methods such as the chorioallantoic membrane assay [1, 2], the monkey iris neovascularization model [3], disk angiogenesis assay [4], and various models using the cornea to assess blood vessel growth [5–10]. These models have played an important role to understand the mechanisms of blood vessel growth and its inhibition.

We recently used a novel transgenic nude mouse for the imaging of human tumor angiogenesis. In this mouse model, the stem cell marker nestin is expressed in nascent blood vessels. A regulatory element of nestin drives green fluorescent protein in this transgenic mouse (ND-GFP), enabling nascent blood vessels to be visualized by their GFP expression. Many human and rodent cancer cell lines expressing red fluorescent protein (RFP) were implanted in the ND-GFP nude mice

¹ To whom correspondence and reprint requests should be addressed at Moores UCSD Cancer Center, 3855 Health Sciences Drive, La Jolla, CA 92093-0987. E-mail: mbouvet@ucsd.edu.

and grew extensively. ND-GFP was highly expressed in proliferating endothelial cells and nascent blood vessels in the growing tumors, visualized by dual-color fluorescence imaging [11]. Doxorubicin inhibited the nascent tumor angiogenesis as well as tumor growth in ND-GFP mice transplanted with the B16F10-RFP murine melanoma [12].

Primary tumor angiogenesis in the ND-GFP transgenic nude mice with orthotopically transplanted MIA PaCa-2 human pancreatic cancer expressing RFP was also visualized by dual-color imaging. Gemcitabine significantly decreased the mean nascent blood vessel density in the tumor as well as decreased tumor volume. These results demonstrated for the first time that gemcitabine is an inhibitor of angiogenesis as well as tumor growth in pancreatic cancer [13].

Angiogenesis of liver metastasis of the XPA-1-RFP human pancreatic cancer in the ND-GFP transgenic nude mice was visualized by dual-color fluorescence imaging. ND-GFP was highly expressed in proliferating endothelial cells and nascent blood vessels in the growing liver metastasis. The density of nascent blood vessels in the liver metastasis was readily quantitated by ND-GFP expression. Gemcitabine significantly decreased the mean nascent blood vessel density in the liver metastases [14].

Orthopedic cancers, such as bone and soft tissue sarcoma, are usually treated by chemotherapy and surgery. However, the efficacy of chemotherapy is highly variable [15–17] and novel effective anticancer agents, such as angiogenesis inhibitors, are needed for this class of disease. Bone metastasis from other tumor types, such as prostate and breast cancer, is very frequent and these metastases are also usually treatment-resistant. Quality of life for these cancer patients depends to a great extent to how bone metastasis is controlled.

Klenke *et al.* [18] reported antiangiogenic efficacy of a Cox-2 inhibitor for a cranial bone tumor model using intravital microscopy. Peyruchaud *et al.* [19] showed that the angiogenesis inhibitor, Angiostatin, inhibited tumor growth in bone by inhibiting osteoclast activity.

In the present study, we have imaged ND-GFP expressing nascent blood vessels vascularizing the HT-1080 human fibrosarcoma expressing RFP, as it formed bone and soft tissue sarcomas. We also demonstrated that angiogenesis of these tumors can be significantly inhibited.

MATERIALS AND METHODS

ND-GFP Transgenic Mice

Transgenic mice carrying GFP under the control of the nestin second-intron enhancer (ND-GFP mice) were originally obtained from Dr. G. Enikolopov (Cold Spring Harbor Laboratory, Cold Spring Harbor, NY) [20, 21].

RFP Vector Production

The RFP (DsRed-2) gene (BD Biosciences Clontech, Palo Alto, CA) was inserted in the retroviral-based mammalian expression vector pLNCX (BD Biosciences Clontech) to form the pLNCX DsRed-2 vector [22]. Production of retrovirus resulted from transfection of pLNCX DsRed-2 into PT67 packaging cells, which produce retroviral supernatants containing the DsRed-2 gene. Briefly, PT67 cells were grown as monolayers in DMEM supplemented with 10% FCS (Gemini Biological Products, Calabasas, CA). Exponentially growing cells (in 10 cm dishes) were transfected with 10 μ g expression vector using a LipofectAMINE Plus (Life Technologies, Inc. Grand Island, NY) protocol. Transfected cells were replated 48 h after transfection and 100 μ g mL⁻¹ G418 was added 7 h after transfection. Two days later, the medium was changed to 200 μ g mL⁻¹ G418. After 25 d of drug selection, surviving colonies were visualized under fluorescence microscopy and RFP-positive colonies were isolated. Several clones were selected and expanded into cell lines after virus titering on the 3T3 cell line.

RFP Gene Transduction of Tumor Cell Lines

For RFP gene transduction, 70% confluent HT-1080 human fibrosarcoma cells were incubated with a 1:1 precipitated mixture of retroviral supernatants of PT67 cells and RPMI 1640 or other culture media (Life Technologies, Inc.) containing 10% fetal bovine serum (Gemini Biological Products) for 72 h. Fresh medium was replenished at this time. Tumor cells were harvested with trypsin/EDTA and subcultured at a ratio of 1:15 into selective medium, which contained 50 μ g/mL G418. To select brightly fluorescent cells, the level of G418 was increased to 800 μ g/mL in a stepwise manner. Clones expressing RFP were isolated with cloning cylinders (Bel-Art Products, Pequannock, NJ) by trypsin/EDTA and were amplified and transferred by conventional culture methods in the absence of selective agent [22].

Transplantation of Tumor Cells

ND-GFP transgenic mice 6 to 8 wk old were used. The mice were anesthetized during the surgery with a ketamine mixture (10 μ L of ketamine HCl, 7.6 μ L of xylazine, 2.4 μ L of acepromazine maleate, and 10 μ L of H₂O) via s.c. injection. Fifty microliters containing 1×10^6 HT-1080 cells were injected in the quadriceps muscle or subcutaneous tissue with a 0.5 mL 28 G latex-free syringe (TYCO Health Group LP, Mansfield, MA). For bone injection, the tibial tuberosity was exposed. Ten microliters containing 1×10^6 cells were injected into the medullary cavity from the tibial tuberosity. The incision in the knee was closed with 6-0 surgical suture in one layer.

On day-7 and day-14 after injection of the tumor, the mice were anesthetized. Tumor samples were excised with the surrounding tissues and were divided into two parts, one for fluorescence microscopy and the other for frozen sections. Tissue was embedded in tissue-freezing embedding medium and frozen at -80°C overnight. Frozen sections 10 μ m thick were cut with a Leica CM1850 cryostat and were air-dried.

Measurement of Length of Nestin-Positive Nascent Blood Vessels and Evaluation of Antiangiogenic Efficacy of Doxorubicin

The mice were treated with 5 mg/kg of doxorubicin (Aldrich, Milwaukee, WI) (ip) or NaCl solution (vehicle controls) at day-0, day-1, and day-2 after subcutaneous, muscular, or bone implantation of tumor cells. Tumor samples were excised under anesthesia at day-8 after implantation of tumor cells. At the end of experiment, the mice were euthanized. The tumors visible with the naked eye were surgically removed. The tumors were measured in three dimensions with calipers. Tumor volume (mm³) was calculated with the formula

$V = 0.52 \times \text{length} \times \text{width} \times \text{height}$. Angiogenesis was quantified in the tumor mass by measuring the total length of ND-GFP-expressing nascent blood vessels under fluorescence microscopy in both doxorubicin-treated and control mice. The tumors were compressed onto a glass slide, enabling the three dimensional vascular structures to be seen in a flattened field using the Olympus OV100 imaging system. Under $100\times$ magnification, the total length of all vessels in all fields within the tumor was then measured with reference to a metric ruler placed adjacent to the tumor. The vessel density at day-8 was calculated by the total length of nestin-positive nascent blood vessels divided by the tumor volume (mm^3). Each experimental group consisted of five mice.

Fluorescence Imaging in Live Mice

The Olympus OV100 small animal imaging system (Olympus Corp., Tokyo, Japan) containing an MT-20 light source (Olympus Biosystems, Planegg, Germany) and DP70 CCD camera (Olympus) was used for imaging in live mice [23]. High-resolution images were captured directly on a PC (Fujitsu Siemens, Munich, Germany). Images were processed for contrast and brightness and analyzed with the use of Paint Shop Pro 8 and CellR (Olympus Biosystems).

Immunohistochemical Staining

Colocalization of ND-GFP fluorescence and CD31 in the frozen skin sections of the nestin-GFP transgenic mice were detected with the antirat immunoglobulin horseradish peroxidase detection kit (CD31; BD PharMingen, San Diego, CA) following the manufacturer's instructions. The primary antibody used was CD31 monoclonal antibody (1:50). Substrate-chromogen 3,3'-diaminobenzidine staining was used for antigen staining. Anti-CD31 monoclonal antibody (CBL1337) was purchased from Chemicon (Temecula, CA).

Statistical Analysis

The experimental data are expressed as the mean \pm SD. Statistical analysis was done using the two-tailed Student's *t*-test.

RESULTS AND DISCUSSION

Tumor Angiogenesis Visualized by ND-GFP

At day-7 or day-14 after implantation of RFP-expressing HT-1080 human fibrosarcoma cells into the muscle or bone of ND-GFP transgenic nude mice, tumors were excised and flattened on a glass slide. The vascular structures were not disrupted by this process. This technique enabled imaging of angiogenesis throughout the tumor. ND-GFP-expressing blood vessels were seen in each type of sarcoma. Newly formed ND-GFP-expressing blood vessels were observed growing into the RFP-expressing tumor mass (Fig. 1, Fig. 2).

We observed early angiogenesis in bone and soft tissue tumor. Comparing the number of new vessels, angiogenesis in muscle was more frequent than in bone at day-14 after tumor implantation. There are many small vessels in muscle and these may be able to initiate angiogenesis more rapidly than in the bone. The soft tissue of muscle may be more conducive to angiogenesis than hard bone structures.

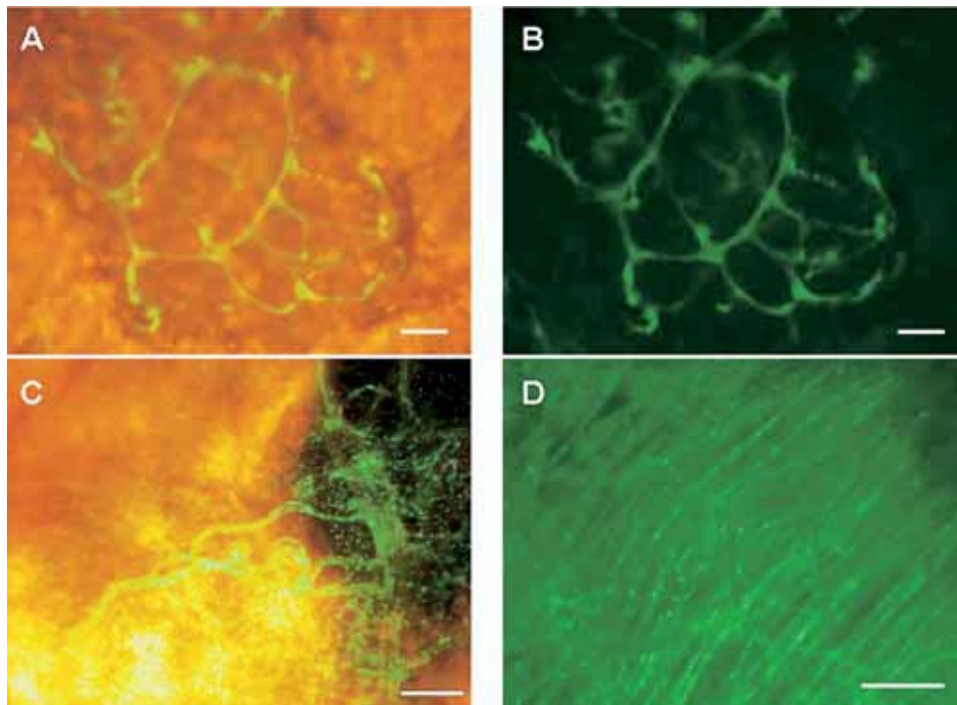


FIG. 1. Angiogenesis of soft tissue sarcoma in muscle. Imaging was carried out at day-14 after implantation of RFP-expressing HT-1080 human fibrosarcoma cells into the quadriceps muscle of ND-GFP transgenic nude mice. (A) ND-GFP-expressing blood vessels are seen in the RFP-expressing tumor. The vessel structures appear irregular compared with normal vessels. (B) Same as (A) but showing only GFP fluorescence. (C) Newly formed ND-GFP-expressing blood vessels are seen growing into the RFP-expressing tumor mass. (D) Blood vessels in normal muscle without tumor. Bars: 50 μm (A), (B) and 200 μm (C), (D).

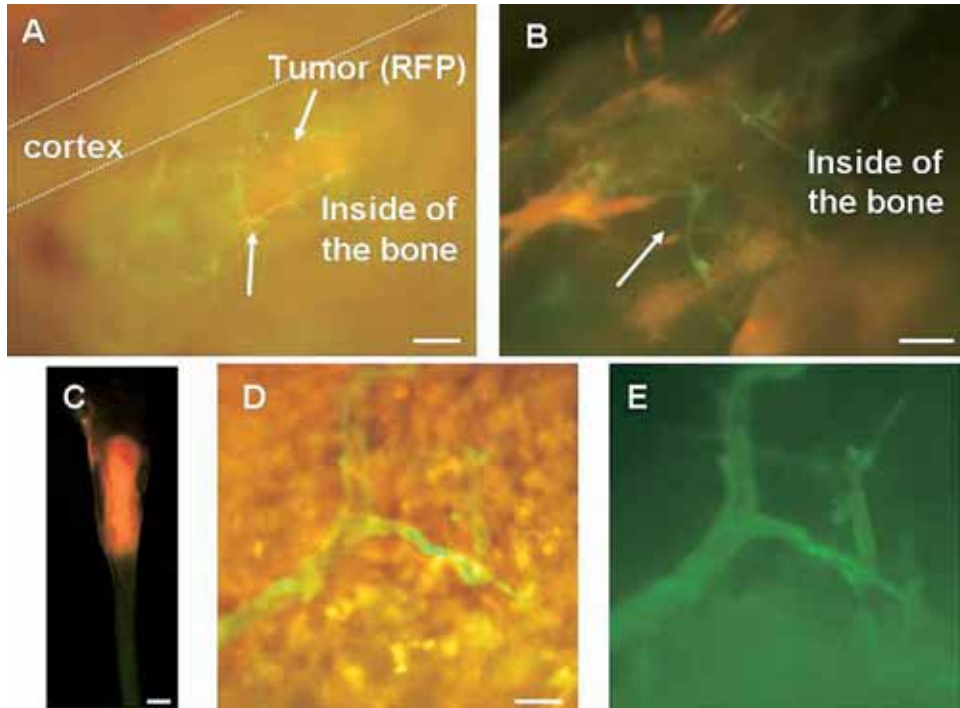


FIG. 2. Angiogenesis of sarcoma in bone. (A) and (B) Dual-color imaging was carried out at day-7 after implantation of RFP-expressing HT-1080 human fibrosarcoma cells into the tibia of ND-GFP transgenic nude mice. Newly-formed vessels formed a network around the RFP-expressing tumor. (C) At day-14, the RFP tumor mass is seen in the tibia. (D) At day-14, ND-GFP-expressing blood vessels are seen in the RFP-expressing tumor. (E) Same as (A) but showing only GFP fluorescence. Bars: (A) 100 μm ; (B) 50 μm ; (C) 1 mm; (D) and (E) 50 μm .

CD 31 is an epithelial marker that is commonly used to identify tumor vessels. Immunohistochemical staining showed that CD31 colocalized in the blood vessels

in the growing sarcomas. Frozen sections showing the ND-GFP blood vessels and RFP-expressing HT-1080 fibrosarcoma under fluorescence microscopy were com-

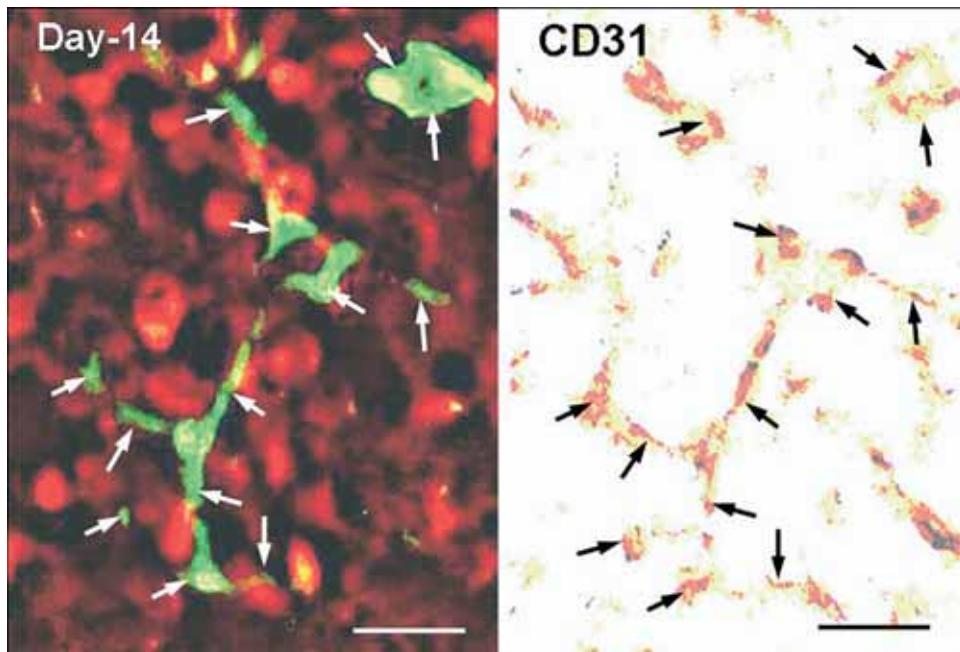


FIG. 3. Immunohistochemical staining of CD31. (A) ND-GFP is visualized in blood vessels in the HT-1080 tumor in a frozen section. (B) Immunohistochemical staining in a sister frozen section shows CD31 co-localizing with ND-GFP in blood vessels in the growing tumor. Bars: 25 μm .

TABLE 1

Doxorubicin Reduced Tumor Volume in Sarcomas Implanted into the Subcutaneous Tissues, Muscle, or Bone of ND-GFP Transgenic Nude Mice

Implantation site	Subcutaneous		Muscle		Bone	
	NaCl	Dox	NaCl	Dox	NaCl	Dox
Average tumor volume (mm ³)	49.8	4.2	22.9	4.2	3.4	0.1
Standard deviation	16.4	3.2	14.1	6.5	1.4	0.1
<i>t</i> -Test	0.0003		0.026		0.038	

Dox = doxorubicin.

pared with sister sections stained for CD31, demonstrating colocalization of ND-GFP and CD-31 (Fig. 3).

Comparison of Immature and Mature Vessels for Blood Flow

At day-14, sarcoma grown in the muscle was exposed with an incision above the quadriceps under anesthesia. Mature and immature blood vessels were observed with the OV100 small-animal imaging system. Immature blood vessels without blood flow had strong nestin-GFP expression. Mature vessels with blood flow had less nestin expression (data not shown).

Effects of Doxorubicin on Tumor Growth and Angiogenesis

Mice were given daily i.p. injections 5 mg/kg of doxorubicin at days -0, -1, and -2 after implantation of the HT-1080 human fibrosarcoma cells into the subcutaneous tissues, muscle, or bone. This protocol was used to minimize doxorubicin toxicity. At day-8 after implan-

tation, the number of ND-GFP-expressing blood vessels was significantly reduced in the doxorubicin-treated animals than in NaCl-injected control mice. Treatment with doxorubicin significantly decreased tumor volume as well as nascent blood vessel formation at each site of tumor implantation (Table 1). Mean nascent blood vessel length per tumor volume was also decreased (Fig. 4; **P* < 0.05 versus NaCl solution-injected mice).

The model described in this study has several advantages over other *in vivo* models of angiogenesis such as the chorioallantoic membrane assay [1, 2], the monkey iris neovascularization model [3], disk angiogenesis assay [4], and various models using the cornea to assess blood vessel growth [5–10]. These advantages include the ability to measure angiogenesis when tumor is implanted orthotopically into its native milieu. We and others have demonstrated that orthotopic or “same

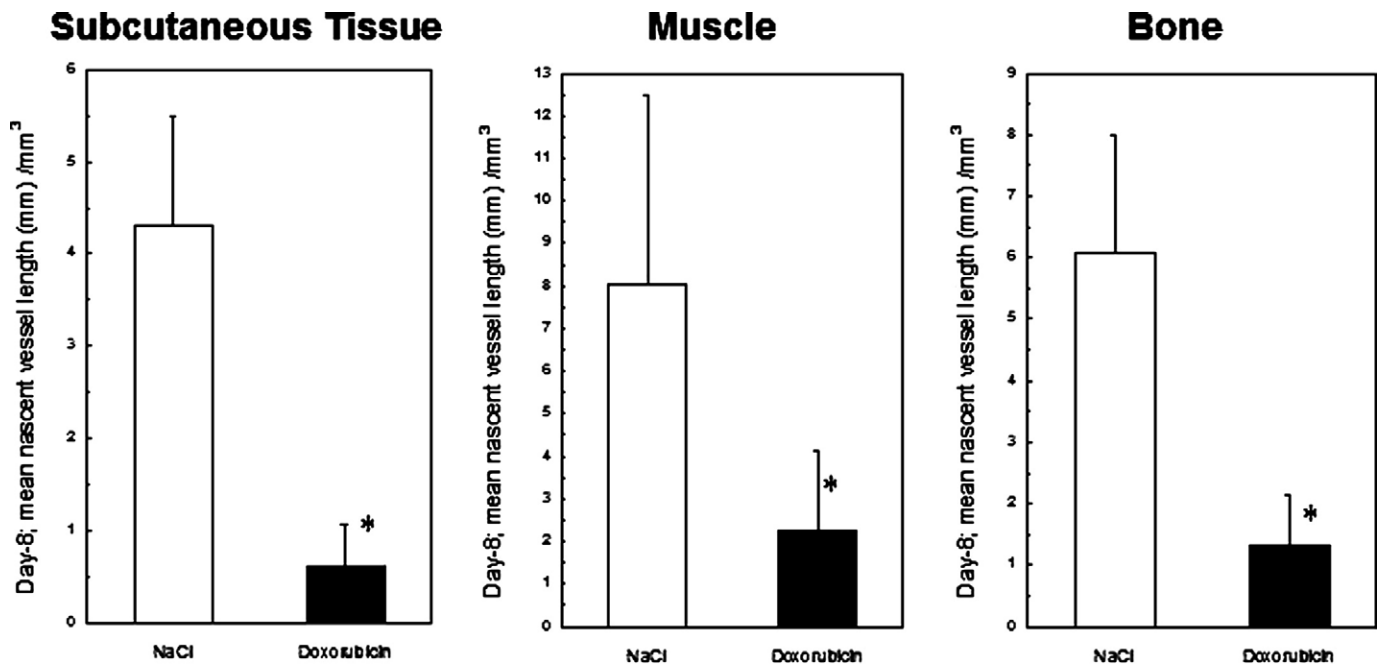


FIG. 4. Efficacy of doxorubicin on angiogenesis. At day-8 after implantation of tumor cells into the subcutaneous tissues, muscle, or bone; doxorubicin significantly decreased the mean nascent blood vessel length per tumor area. **P* < 0.001 versus NaCl solution-injected mice.

site" implantation more closely resembles the clinical state of tumor growth and metastasis [24].

The model does have several limitations as well. For instance, the quantitation of vessel density was determined *ex vivo* in tumors that were harvested after euthanizing animals. Our future studies are focused on developing models in which angiogenesis can be quantitated in real time without the need for sacrificing the animal. Also, we have not yet performed studies looking at changes in blood vessel density over time but plan to do so in future studies.

In conclusion, these results show the utility of the dual-color ND-GFP mouse RFP soft tissue-tissue sarcoma model to visualize and quantitate angiogenesis. The dual-color model described here should be very useful to screen and evaluate potential new angiogenesis inhibitors that inhibit soft tissue and bone sarcoma, a disease that is currently highly treatment-resistant.

ACKNOWLEDGMENTS

This work was supported by NIH grant R21 CA109949-01 and the American Cancer Society RSG-05-037-01-CCE (MB) and National Cancer Institute grants CA099258, CA103563, and CA101600 (to AntiCancer, Inc.).

REFERENCES

1. Auerbach R, Kubai L, Knighton D, et al. A simple procedure for the long-term cultivation of chicken embryos. *Dev Biol* 1974;41:391.
2. Crum R, Szabo S, Folkman J. A new class of steroids inhibits angiogenesis in the presence of heparin or a heparin fragment. *Science* 1985;230:1375.
3. Miller JW, Stinson WG, Folkman J. Regression of experimental iris neovascularization with systemic α -interferon. *Ophthalmology* 1993;100:9.
4. Passaniti A, Taylor RM, Pili R, et al. A simple, quantitative method for assessing angiogenesis and antiangiogenic agents using reconstituted basement membrane, heparin, and fibroblast growth factor. *Lab Invest* 1992;67:519.
5. Alessandri G, Raju K, Gullino PM. Mobilization of capillary endothelium *in vitro* induced by effectors of angiogenesis *in vivo*. *Cancer Res* 1983;43:1790.
6. Deutsch TA, Hughes WF. Suppressive effects of indomethacin on thermally induced neovascularization of rabbit corneas. *Am J Ophthalmol* 1979;87:536.
7. Epstein RJ, Hendricks RL, Stulting RD. Interleukin-2 induces corneal neovascularization in A/J mice. *Cornea* 1990;9:318.
8. Korey M, Peyman GA, Berkowitz R. The effect of hypertonic ointments on corneal alkali burns. *Ann Ophthalmol* 1977;9:1383.
9. Li WW, Grayson G, Folkman J, et al. Sustained release endotoxin. A model for inducing corneal neovascularization. *Invest Ophthalmol Vis Sci* 1991;32:2906.
10. Mahoney JM, Waterbury LD. Drug effects on the neovascularization response to silver nitrate cauterization of the rat cornea. *Curr Eye Res* 1985;4:531.
11. Amoh Y, Yang M, Li L, et al. Nestin-linked green fluorescent protein transgenic nude mouse for imaging human tumor angiogenesis. *Cancer Res* 2005;65:5352.
12. Amoh Y, Li L, Yang M, et al. Hair follicle-derived blood vessels vascularize tumors in skin and are inhibited by doxorubicin. *Cancer Res* 2005;65:2337.
13. Amoh Y, Li L, Tsuji K, et al. Dual-color imaging of nascent blood vessels vascularizing pancreatic cancer in an orthotopic model demonstrates antiangiogenesis efficacy of gemcitabine. *J Surg Res* 2006;132:164.
14. Amoh Y, Nagakura C, Maitra A, et al. Dual-color imaging of nascent angiogenesis and its inhibition in liver metastases of pancreatic cancer. *Anticancer Res* 2006;26:3237.
15. Bielack SS, Kempf-Bielack B, Delling G, et al. Prognostic factors in high-grade osteosarcoma of the extremities or trunk: An analysis of 1702 patients treated on neoadjuvant cooperative osteosarcoma study group protocols. *J Clin Oncol* 2002;20:776.
16. Tsuchiya H, Tomita K, Mori Y, et al. Marginal excision for osteosarcoma with caffeine assisted chemotherapy. *Clin Orthop Relat Res* 1999;358:27.
17. Tsuchiya H, Tomita K, Yamamoto N, et al. Caffeine-potentiated chemotherapy and conservative surgery for high-grade soft-tissue sarcoma. *Anticancer Res* 1998;18:3651.
18. Klenke FM, Gebhard MM, Ewerbeck V, et al. The selective Cox-2 inhibitor Celecoxib suppresses angiogenesis and growth of secondary bone tumors: An intravital microscopy study in mice. *BMC Cancer* 2006;6:9.
19. Peyruchaud O, Serre CM, NicAmhlaioibh R, et al. Angiostatin inhibits bone metastasis formation in nude mice through a direct antiosteoclastic activity. *J Biol Chem* 2003;278:45826.
20. Amoh Y, Li L, Yang M, et al. Nascent blood vessels in the skin arise from nestin-expressing hair-follicle cells. *Proc Natl Acad Sci USA* 2004;101:13291.
21. Li L, Mignone J, Yang M, et al. Nestin expression in hair follicle sheath progenitor cells. *Proc Natl Acad Sci USA* 2003;100:9958.
22. Yang M, Li L, Jiang P, et al. Dual-color fluorescence imaging distinguishes tumor cells from induced host angiogenic vessels and stromal cells. *Proc Natl Acad Sci USA* 2003;100:14259.
23. Yamauchi K, Yang M, Jiang P, et al. Development of real-time subcellular dynamic multicolor imaging of cancer-cell trafficking in live mice with a variable-magnification whole-mouse imaging system. *Cancer Res* 2006;66:4208.
24. Hoffman RM. Orthotopic metastatic mouse models for anticancer drug discovery and evaluation: a bridge to the clinic. *Invest New Drugs* 1999;17:343.